Common variants associated with *OSMR* expression contribute to carotid plaque vulnerability, but not to cardiovascular disease in humans

Authors
D. van Keulen, MSc[1,2,3,4], I. D. van Koeverden, MD PhD[1], A. Boltjes PhD[2], H. M. G. Princen, PhD[4], A. J. van Gool, PhD[5,6], G.J. de Borst, MD PhD[7], F.W. Asselbergs, MD PhD[8,9,10], D. Tempel, PhD[2,3,11], G. Pasterkamp, MD PhD[2]*, S.W. van der Laan, PhD[2]*.
* these authors contributed equally

Affiliations
[1]Laboratory of Experimental Cardiology, University Medical Center Utrecht, University of Utrecht, Utrecht, The Netherlands;
[2]Laboratory of Clinical Chemistry and Hematology, University Medical Center Utrecht, University of Utrecht, Utrecht, The Netherlands;
[3]Quorics B.V., Rotterdam, The Netherlands;
[4]TNO-Metabolic Health Research, Gaubius Laboratory, Leiden, The Netherlands;
[5]Translational Metabolic Laboratory, Radboudumc, Nijmegen, The Netherlands;
[6]TNO- Microbiology & Systems Biology, Zeist, The Netherlands;
[7]Department of Vascular Surgery, University Medical Center Utrecht, University of Utrecht, Utrecht, The Netherlands;
[8]Department of Cardiology, Division Heart & Lungs, University Medical Center Utrecht, Utrecht University, Utrecht, The Netherlands;
[9]Institute of Cardiovascular Science, Faculty of Population Health Sciences, University College London, London, United Kingdom;
[10]Health Data Research UK and Institute of Health Informatics, University College London, London, United Kingdom
[11]SkylineDx B.V., Rotterdam, The Netherlands.

Corresponding authors
Prof. dr. G. Pasterkamp
Laboratory of Clinical Chemistry, Division Laboratories, Pharmacy, and Biomedical Genetics, University Medical Center Utrecht, Utrecht University
Heidelberglaan 100, 3508 GA, Utrecht, the Netherlands
Telephone: +31 (0) 88 75 571 55
Fax: +31 (0)30 252 26 93
E-mail: g.pasterkamp@umcutrecht.nl

dr. S.W. van der Laan
Laboratory of Clinical Chemistry, Division Laboratories, Pharmacy, and Biomedical Genetics, University Medical Center Utrecht, Utrecht University
Heidelberglaan 100, 3508 GA, Utrecht, the Netherlands
Telephone: +31 (0) 88 75 676 96
Fax: +31 (0)30 252 26 93
E-mail: s.w.vanderlaan-2@umcutrecht.nl

Journal subject terms
Epigenetics, Genetics, Atherosclerosis, Cardiovascular disease

2 Tables, 2 Figures, 3 supplemental tables, 2 supplemental figures

Background and aims
Oncostatin M (OSM) signaling is implicated in atherosclerosis, however the mechanism remains unclear. We investigated the impact of common genetic variants in *OSM* and its receptors, *OSMR* and *LIFR,* on overall plaque vulnerability, plaque phenotype, intraplaque *OSMR* and *LIFR* expression, coronary artery calcification burden and cardiovascular disease susceptibility.

Methods and results
We queried Genotype-Tissue Expression data and found rs13168867 (C allele) and rs10491509 (A allele) to be associated with decreased *OSMR* and increased *LIFR* expression in arterial tissue respectively. No variant was significantly associated with *OSM* expression.

We associated these two variants with plaque characteristics from 1,443 genotyped carotid endarterectomy patients in the Athero-Express Biobank Study. rs13168867 was associated with an increased overall plaque vulnerability (β=0.118 ± s.e.=0.040, p=3.00x10^{-3}, C allele) and although not significant after correction for multiple testing, it showed strongest associations with intraplaque fat (β=0.248 ± s.e.=0.088, C allele) and collagen content (β=-0.259 ± s.e.=0.095, C allele). rs13168867 was not associated with intraplaque *OSMR* expression. Neither was intraplaque *OSMR* expression associated with plaque vulnerability and no known *OSMR* eQTLs were associated with coronary artery calcification burden, or cardiovascular disease susceptibility. No associations were found for rs10491509 in the *LIFR* locus.

Conclusions
Our study suggests that genetically decreased arterial *OSMR* expression contributes to increased carotid plaque vulnerability. However, the OSM signaling pathway is unlikely to be causally involved in lifetime cardiovascular disease susceptibility as none of the investigated variants associated with cardiovascular diseases.

Keywords: Atherosclerosis, plaque, OSM, OSMR

1. Introduction

The prevalence of cardiovascular disease (CVD) is high, poses a significant global burden and is expected to rise[1]. Arterial inflammation, leading to asymmetric focal arterial thickening and atherosclerotic plaque formation and progression, is the primary mechanism underlying CVD[2]. Inflammatory cytokines contribute to arterial inflammation and subsequent atherosclerotic plaque formation[3]. One cytokine, for which there is mounting evidence suggesting a role in atherosclerosis development is OSM[4,5]. It has been shown that OSM is present in both murine and human atherosclerotic plaques[6]. Moreover, murine studies showed that OSM receptor (OSMR)$^{-/-}$ApoE$^{-/-}$ mice have reduced plaque size and improved plaque stability compared to their *OSMR*-expressing littermates[7], indicating that OSM drives atherosclerosis development. These observations are in line with our previous work, in which we showed that simultaneous signaling of OSM through OSMR and leukemia inhibitory factor receptor (LIFR), induces activation in human endothelial cells, suggestive of a role in atherosclerosis development[8]. In contrast, chronic OSM administration to APOE*3Leiden.CETP mice reduces the atherosclerotic lesion size and severity, and high circulating OSM levels correlate with increased post-incident coronary heart disease survival probability in humans[9].

Although all these studies implicate that OSM is involved in atherosclerosis, little is known about the effects of OSM on plaque composition in humans. Grouped in the interleukin 6 subfamily of cytokines, OSM is released by activated immune cells[10–12], and exerts pleiotropic effects on cell proliferation, inflammation, hematopoiesis, tissue remodeling, and development[13]. Its signals are transduced through binding to either OSMR or LIFR, which form a heterodimer with glycoprotein 130[8,14], that in turn activates multiple pathways[14]. It is suggested that the ratio of the two receptor types expressed on the cell membrane is a potential regulatory mechanism for the multiple, and sometimes opposing, effects that are exerted by OSM[15].

Thus, given its pleiotropic function, it is difficult to predict how OSM contributes to atherosclerotic plaque formation. Cell and murine studies have shown that OSM promotes angiogenesis[4], endothelial activation[8], vessel permeability[16], and osteoblastic differentiation[17]. Therefore, increased OSM levels hypothetically results in a higher intraplaque microvessel density, intraplaque hemorrhages and plaque calcification, thereby contributing to plaque destabilization[18,19]. In other cell and murine studies, OSM promotes fibroblast proliferation[20], collagen formation[20], smooth muscle cell proliferation[6], and M2 macrophage polarization[21]. These processes hypothetically lead to enhanced fibrosis, and attenuated inflammation, thereby contributing to plaque stabilization[22].

Large-scale studies have shown that *cis*-acting genetic variants associated to gene expression (expression quantitative trait loci (eQTLs)[23]) are key to disease susceptibility[24]. This means that gene expression differs between individuals carrying different genotypes (for example AA, Aa, aa) for a given eQTL in a given tissue which ultimately results in differential disease susceptibility. Thus, on the premise that alleles are randomly distributed at conception and are invariant throughout a lifetime, meaning that genetics is not influenced by disease or risk factors, eQTLs can be used as proxies of gene expression to examine the effect on plaque morphology[25]. We hypothesized that if *OSM*, *OSMR*, or *LIFR* expression has an effect on plaque morphology, these phenotypic differences will be observed among genotype groups of the eQTL. We aimed to investigate the double-edged sword of OSM signaling on the composition of human atherosclerotic plaques using known eQTLs of *OSM*, *OSMR*, and *LIFR*.

2. Materials and methods

2.1 Sample collection

The Athero-Express Biobank Study (https://www.atheroexpress.nl) is an ongoing prospective study, containing biomaterial of patients elected for endarterectomy at two Dutch tertiary referral centers. Details of the study design were described before[26]. Briefly, blood subfractions and arterial plaque material are obtained during endarterectomy. Each plaque is dissected into segments of 0.5cm. The culprit lesion is reserved for histological assessment (see below), while surrounding segments are immediately snap frozen in liquid nitrogen and stored at -80°C for later use, e.g. in order to perform RNA-seq (see below). Only carotid endarterectomy (CEA) patients were included in the present study. All research was conducted according to the principles of the Declaration of Helsinki and its later amendments, all patients provided informed consent and the study was approved by the medical ethics committee.

2.2 Athero-Express genotyping, quality control, and imputation

Details of genotyping were previously described[26]. Briefly, DNA was extracted from EDTA blood or (when no blood was available) plaque samples of 1,858 consecutive patients from the Athero-Express Biobank Study and genotyped in 2 batches. For the Athero-Express Genomics Study 1 (AEGS1), 836 patients, included between 2002 and 2007, were genotyped using the Affymetrix Genome-Wide Human SNP Array 5.0 (SNP5) chip (Affymetrix Inc., Santa Clara, CA, USA). For the Athero-Express Genomics Study 2 (AEGS2), 1,022 patients, included between 2002 and 2013 and not overlapping AEGS1, were genotyped using the Affymetrix Axiom® GW CEU 1 Array (AxM). Both studies were carried out according to OECD standards. After genotype calling, we adhered to community standard quality control and assurance (QA/QA) procedures of the genotype data from AEGS1 and AEGS2. Samples with low average genotype calling and sex discrepancies (compared to the clinical data available) were excluded. The data was further filtered on 1) individual (sample) call rate >97%, 2) SNP call rate >97%, 3) minor allele frequencies (MAF) >3%, 4) average heterozygosity rate ± 3.0 s.d., 5) relatedness (pi-hat >0.20), 6) Hardy–Weinberg Equilibrium (HWE $p < 1.0 \times 10^{-6}$), and 7) population stratification (based on HapMap 2, release 22, b36) by excluding samples deviating more than 6 standard deviations from the average in 5 iterations during principal component analysis and by visual inspection as previously described[26]. After QA/QA, 657 samples and 403,789 SNPs in AEGS1, and 869 samples and 535,983 SNPs in AEGS2 remained. Before phasing using SHAPEIT2[27], data was lifted to genome build b37 using the liftOver tool from UCSC (https://genome.ucsc.edu/cgi-bin/hgLiftOver). Finally, data was imputed with 1000G phase 3[28] and GoNL 5[29] as a reference.

2.3 Variant selection

We queried data from the Genotype-Tissue Expression (GTEx) Portal (https://gtexportal.org)[23] for variants that alter *OSM* expression in blood, and *OSMR* or *LIFR* expression in non-diseased arterial tissue. We selected common variants with a MAF >3%, which yielded 2 variants in total. We harmonized the effect alleles and effect sizes from these eQTLs to match the allele orientation in the Athero-Express Biobank Study data.

2.4 Plaque phenotyping

The (immuno)histochemical analysis of plaques have been described previously[26,30,31]. Briefly, per plaque, the culprit lesion was identified directly after dissection, fixed in 4% formaldehyde, embedded in paraffin and cut in 5µm sections on a microtome for (immuno)histochemical analysis by pathology experts. Calcification (hematoxylin & eosin, H&E) and collagen content (picrosirius red) were semi-quantitatively scored and defined as no/minor or moderate/heavy. Atheroma size (H&E and picrosirius red) was defined as <10% or ≥10% fat content. Macrophages (CD68) and smooth muscle cells (ACTA2) were quantitatively scored and classified as percentage of plaque area. Intraplaque hemorrhage

(H&E) was defined as absent or present, and vessel density was classified as the number of intraplaque vessels (CD34) per 3-4 hotspots.

2.5 Plaque vulnerability

Assessment of overall plaque vulnerability was performed as previously described[25]. Briefly, macrophages and smooth muscle cells were semi-quantitatively defined as no/minor or moderate/heavy. Each plaque characteristic that defines a stable plaque (i.e. no/minor macrophages, moderate/heavy collagen, moderate/heavy smooth muscle cells and <10% fat) was given a score of 0, while each plaque characteristic that defines a vulnerable plaque (i.e. moderate/heavy macrophages, no/minor collagen, no/minor smooth muscle cells and ≥10% fat) was given a score of 1. The score of each plaque characteristic was summed resulting in a final plaque score ranging from 0 (most stable plaque) to 4 (most vulnerable plaque). Intraobserver and interobserver variability were examined previously and showed good concordance (κ=0.6-0.9)[32].

2.6 Plaque expression

To be able to assess the global expression profile, plaque segments were thawed, cut up, and further homogenized using ceramic beads and tissue homogenizer (Precellys, Bertin instruments, Montigny-le-Bretonneux, France), in the presence of TriPure (Sigma Aldrich), and RNA was isolated according to TriPure manufacturer's protocol. From here, RNA in the aqueous phase was precipitated using isopropanol, and washed with 75% ethanol, and subsequently stored in 75% ethanol for later use or used immediately after an additional washing step with 75% ethanol.

Library preparation

From here, library preparation was performed, adapting the CEL-Seq2 protocol for library preparation[33,34], as described before[35]. After removing ethanol, and air-drying the pellet, primer mix containing 5ng primer per reaction was added, initiating primer annealing at 65°C for 5min. Subsequent RT reaction was performed; first strand reaction for 1h at 42°C, heat inactivated for 10m at 70°C, second strand reaction for 2h at 16°C, and then put on ice until proceeding to sample pooling. The primer used for this initial reverse-transcription (RT) reaction was designed as follows: an anchored polyT, a unique 6bp barcode, a unique molecular identifier (UMI) of 6bp, the 5' Illumina adapter and a T7 promoter, as described[35]. Each sample now contained its own unique barcode, due to the primer used in the RNA amplification making it possible to pool together complementary DNA (cDNA) samples at 7 samples per pool. cDNA was cleaned using AMPure XP beads (Beckman Coulter), washed with 80% ethanol, and resuspended in water before proceeding to the *in vitro* transcription (IVT) reaction (AM1334; Thermo-Fisher) incubated at 37°C for 13 hours. Next, primers were removed by treating with Exo-SAP (Affymetrix, Thermo-Fisher) and amplified RNA (aRNA) was fragmented, and then cleaned with RNAClean XP (Beckman-Coulter), washed with 70% ethanol, air-dried, and resuspended in water. After removing the beads using a magnetic stand, RNA yield and quality in the suspension were checked by Bioanalyzer (Agilent).

cDNA library construction was then initiated by performing an RT reaction using SuperScript II reverse transcriptase (Invitrogen/Thermo-Fisher) according to the manufacturer's protocol, adding randomhexRT primer as random primer. Next, PCR amplification was done with Phusion High-Fidelity PCR Master Mix with HF buffer (NEB, MA, USA) and a unique indexed RNA PCR primer (Illumina) per reaction, for a total of 11-15 cycles, depending on aRNA concentration, with 30 seconds elongation time. PCR products were cleaned twice with AMPure XP beads (Beckman Coulter). Library cDNA yield and quality were checked by Qubit fluorometric quantification (Thermo-Fisher) and Bioanalyzer (Agilent), respectively. Libraries were sequenced on the Illumina Nextseq500 platform; paired end, 2 x 75bp.

Mapping
Upon sequencing, retrieved fastq files were de-barcoded, split into forward and reverse reads. Subsequently, these were mapped making use of Burrows-Wheel aligner (BWA[36]) version 0.7.17-r1188, calling 'bwa aln' with settings -B 6 -q 0 -n 0.00 -k 2 -l 200 -t 6 for R1 and -B 0 -q 0 -n 0.04 -k 2 -l 200 -t 6 for R2, 'bwa sampe' with settings -n 100 -N 100, and a cDNA reference (assembly hg19, Ensembl release 84). Read counts and UMI counts were derived from SAM files using custom perl code, and then gathered into count matrices. Genes were annotated with Ensembl ID's, and basic quality control was performed, encompassing filtering out samples with low gene numbers (<10,000 genes), and read numbers (<18,000 reads). Resulting number of samples: 641, with 60,674 genes (Ensembl ID's), and median of 178,626 reads per sample.

Data analysis
Stability scores, and genotypes for rs10491509 and rs13168867, were added to metadata, upon which this was combined with counts and annotation in a SummarizedExperiment object[37]. Counts were normalized and transformed making use of the variance stabilization transformation function (vst()) in DESeq2[38]. This results in transformed data on a $\log_2$-scale, normalized for library size. Differential expression analysis between stability scores or genotypes was performed using DESeq2. To test for statistical difference when comparing intraplaque *OSMR* expression of the more vulnerable plaques to the least vulnerable plaque, a multinomial logistic regression analysis was performed.

2.7 Genetic analyses
Quantitatively scored characteristics (macrophages, smooth muscle cells, and the vessel density) were Box-Cox transformed[39] to obtain a normal distribution. For genetic analyses we used GWASToolKit (https://swvanderlaan.github.io/GWASToolKit/) which is a wrap-around collection of scripts for SNPTEST[40]. Continuous and categorical variables were tested using linear and logistic regression models, respectively. Models for genetic analyses were corrected for age, sex, genotyping chip, and genetic ancestry using principal components 1 through 4.

2.8 Multiple testing and power
Correction for multiple testing resulted in a corrected p-value of p=0.05/((7 plaque phenotypes + plaque vulnerability) x 2 common variants)=3.13×10^{-3}. The power of the study was estimated at ±75% based on a sample size of 1,443, a minor allele frequency (MAF) of 0.409 and a relative risk of 1.28 (http://csg.sph.umich.edu/abecasis/cats/gas_power_calculator/).

2.9 Data and scripts
Data is available upon request. Scripts are posted at GitHub https://github.com/swvanderlaan/2019_vankeulen_d_osmr.

3. Results

3.1 Baseline characteristics

A total of 1,443 patients that underwent carotid endarterectomy were genotyped and included in this study. As we previously showed that the baseline characteristics between the two genotyping groups (AEGS1 and AEGS2) are comparable[26], we combined these groups for overall plaque vulnerability and phenotype analyses. Baseline characteristics of the combined groups are shown in **Table 1**.

3.2 Common variants altering *OSM*, *OSMR* and *LIFR* expression

OSM is secreted by, among others, neutrophils[12], monocytes[11], macrophages[11] and T-cells[10], and acts through binding to OSMR and LIFR[14,41,42] in the arterial wall[7,43]. Thus we queried data from the Genotype-Tissue Expression project (GTEx)[23] for SNPs that alter *OSM* expression in whole blood and *LIFR* and *OSMR* expression in arterial tissue. There were no significant eQTLs for *OSM*, but there were two eQTLs associated with altered *OSMR* (rs13168867) or *LIFR* (rs10491509) expression in arterial tissue. The C allele of rs13168867 is associated with decreased *OSMR* expression in the tibial artery (**Figure 1A**), and the A allele of rs10491509 is associated with increased *LIFR* expression in the aortic artery (**Figure 1B**). Cross-tissue meta-analysis showed that these variants have m-values >0.9 in both tibial and aortic artery tissue, indicating a high posterior probability that they are single *cis*-eQTLs in both tissues (**Supplemental Figure 1** and **2**).

3.3 Genetic association with plaque vulnerability

To determine the effect of OSM signaling on the overall plaque vulnerability, we correlated the rs13168867 and rs10491509 genotypes to the overall plaque vulnerability, which was given a score ranging from 0 (least vulnerable plaque) to 4 (most vulnerable plaque). The effect allele of variant rs13168867 in the *OSMR* locus was significantly correlated with an increased overall plaque vulnerability (β=0.118 ± s.e.=0.040 (C allele), p=3.00x10^{-3}, **Figure 2**). No association was observed with rs10491509 and overall plaque vulnerability.

3.4 Genetic association with plaque phenotypes

To determine the effect of OSM signaling on the individual plaque characteristics comprising the overall plaque vulnerability, we assessed the association between rs13168867 and rs10491509 and seven plaque phenotypes in the Athero-Express Biobank Study. Although not significant after correction for multiple testing, the strongest associations were observed between the effect allele of variant rs13168867 in the *OSMR* locus and intraplaque fat (β=0.248 ± s.e.=0.088 (C allele), p=4.66x10^{-3}), and collagen content (β=-0.259 ± s.e.=0.095 (C allele), p=6.22x10^{-3}, **Table 2**). No associations were observed between rs10491509 and any of the plaque phenotypes.

3.5 Known eQTLs of *OSMR* and *LIFR* expression in non-diseased arterial tissue are not associated with expression in atherosclerotic plaques

Atherosclerotic disease progression changes the artery-specific transcriptional dynamics, and may therefore abolish the effects of known *OSMR* and *LIFR* eQTLs in non-atherosclerotic arterial tissues. Thus, we tested whether these eQTLs were associated with *OSMR* and *LIFR* expression in carotid atherosclerotic plaques. Neither variant showed associations with expression of *OSM*, *OSMR*, and *LIFR* (**Supplementary table 1**).

3.6 Intraplaque *OSMR* expression is not associated with plaque vulnerability

As rs13168867 was associated with an increased overall plaque vulnerability, we next investigated if intraplaque *OSMR* expression levels associated with overall plaque vulnerability. Differential expression analyses, comparing the reference score (0) with each increasing vulnerability score (1, 2, 3, or 4) showed no associations between *OSMR* plaque expression levels and plaque vulnerability (**Supplemental Table 2**). Neither did intraplaque *OSM* or *LIFR* expression associate with plaque severity.

3.7 Known eQTLs of *OSMR* and *LIFR* do not associate with cardiovascular diseases

The Athero-Express comprises patients with advanced stage atherosclerotic plaques. Therefore, we assessed the effect of known *OSMR* and *LIFR* eQTLs on coronary calcification (CAC) as intermediate phenotypes of atherosclerotic burden, and primary cardiovascular outcomes as clinical manifestation. We queried summary statistics from GWAS on CAC (n=2,674)[44], coronary artery disease (CAD, n=336,755)[44,45], and ischemic stroke subtypes (sample sizes 242,573-522,258)[44–46]. Neither eQTL associated with increased CAC burden, or cardiovascular disease susceptibility (**Supplemental Table 3**).

4. Discussion

We investigated whether common variants associated to gene expression, i.e. eQTLs, near *OSM, OSMR* and *LIFR* affect overall plaque vulnerability and phenotype. We showed that one *cis*-acting eQTL (rs13168867, C/T), of which the C allele associates with reduced *OSMR* expression in non-diseased arterial tissue, associates with increased plaque vulnerability. This suggests that a decrease in *OSMR* expression and therefore possibly a decrease in OSM signaling, increases the chance of developing a vulnerable plaque.

To gain further insight into the role of genetically decreased *OSMR* expression on developing a vulnerable plaque, we examined the effect of rs13168867 on individual plaque characteristics in more detail. The strongest associations were found for rs13168867 with increased intraplaque fat and decreased collagen content, suggesting that reduced OSM signaling results in a larger lipid core and less fibrosis - in line with a more vulnerable plaque phenotype. We previously showed that OSM enhances ICAM-1 expression on human endothelial cells[8]. Reduced *OSMR* expression, which hypothetically results in reduced OSM signaling, may therefore result in reduced ICAM-1 expression. ICAM-1 depletion leads to M1 macrophage polarization[47], which is the pro-inflammatory macrophage subtype that promotes an unstable plaque phenotype[48]. Reduced OSM signaling could also explain the decreased collagen content as OSM enhances *in vitro* fibroblast proliferation and collagen formation[20]. Moreover, it was previously shown that OSM enhances liver fibrosis in mice[49] and that OSM is upregulated in patients with pulmonary fibrosis[50]. A reduction in OSM signaling caused by decreased OSMR expression may therefore result in decreased collagen content. Further studies are needed to investigate these hypotheses.

A possible explanation for the lack of associations for the variant (rs10491509) in the *LIFR* locus could be that an increase in *LIFR* expression would not affect OSM signaling as, hypothetically, there might already be a *LIFR* surplus and therefore, an increase in *LIFR* expression will not affect OSM signaling.

Although rs13168867 did associate with plaque vulnerability, no associations were found between rs13168867 and intraplaque *OSMR* expression, intraplaque *OSMR* expression and plaque vulnerability, nor did known *OSMR* eQTLs associate with cardiovascular disease outcomes. Possibly, OSM signaling mainly affects atherogenesis and atherosclerosis development in the initial phases of the disease. Arterial *OSMR* expression is reduced in human atherosclerotic plaques when compared to normal arteries[9] and may therefore have bigger effects in the initial phase, when *OSMR* expression is still high. Another possible explanation is that OSM signaling may be overruled by for example, other cytokines in later stages of the disease.

Compared to genome-wide association studies that include thousands of individuals, the Athero-Express Biobank Study is relatively small (n=1,443), and, given its design, finite in size. However, it is well suited to examine the effect of common disease-associated genetic variation on plaque morphology and characteristics. Indeed, we estimated the power at ±75% given a MAF=0.40 (approximately the frequency of rs13168867) and relative risk=1.28 (http://csg.sph.umich.edu/abecasis/gas_power_calculator/).

Recent developments in single-cell expression analyses might extend on the present study by investigating which cell types, that are present in the plaque, most abundantly express *OSM, OSMR* and *LIFR.* Furthermore, it would be interesting to investigate if the *OSMR/LIFR* expression ratio correlates with plaque vulnerability and if this ratio might be a predictor of plaque vulnerability.

5. Conclusion

Based on this work we conclude that the variant rs13168867 in the *OSMR* locus is associated with increased plaque vulnerability, but not with coronary calcification or cardiovascular disease susceptibility. Given the multiple testing burden for individual plaque characteristics, it remains unclear through which precise biological mechanisms OSM

signaling exerts its effects on plaque morphology, although our data point towards lipid metabolism and extracellular matrix remodeling. However, the OSM-OSMR/LIFR pathway is unlikely to be causally involved in lifetime cardiovascular disease susceptibility as none of the investigated eQTLs associated with cardiovascular diseases.

Conflict of interest

DvK is employed by Quorics B.V., and DT is employed by SkylineDx B.V and Quorics B.V. Quorics B.V. and SkylineDx B.V. had no part whatsoever in the conception, design, or execution of this study, nor the preparation and contents of this manuscript.

Financial support

SWvdL is funded through grants from the Netherlands CardioVascular Research Initiative of the Netherlands Heart Foundation (CVON 2011/B019 and CVON 2017-20: Generating the best evidence-based pharmaceutical targets for atherosclerosis [GENIUS I&II]). This work was supported by ERA-CVD, grant number: 01KL1802. FWA is supported by UCL Hospitals NIHR Biomedical Research Centre. DvK, HP and DT are funded through the FP7 EU project CarTarDis (FP7/2007-2013) under grant agreement 602936. HP received funding from the TNO research program "Preventive Health Technologies". The funding sources were not involved in study design, collection, analysis and interpretation of data, writing of the report and in the decision to submit the article for publication.

Author contributions

DvK: Conceptualization, Formal analysis, Writing - original draft. IvK: Data curation. AB: Conceptualization, Formal analysis, Writing – review & editing. HP: Writing – review & editing. AvG: Writing – review & editing. GJdB: Conceptualization. FA: Conceptualization. DT: Conceptualization, Writing – review & editing. GP: Conceptualization, Writing – review & editing. SvdL: Conceptualization, Formal analysis, Writing – original draft, review & editing.

Acknowledgments

We would like to thank dr. Jessica van Setten and acknowledge her for imputing our datasets using an in-house developed imputation pipeline. Evelyn Velema and Petra Homoet-Van der Kraak are acknowledged for the immunohistochemical stainings. We also acknowledge the support from the Netherlands CardioVascular Research Initiative from the Dutch Heart Foundation, Dutch Federation of University Medical Centres, the Netherlands Organisation for Health Research and Development and the Royal Netherlands Academy of Sciences ("GENIUS I & II", CVON2011-19) and the TNO research program "Preventive Health Technologies".

References

1. Moodie, D. S. The Global Burden of Cardiovascular Disease. *Congenit. Heart Dis.* **11**, 213–213 (2016).
2. Hansson, G. K. Inflammation, atherosclerosis, and coronary artery disease. *New England Journal of Medicine* vol. 352 (2005).
3. Sprague, A. H. & Khalil, R. A. Inflammatory cytokines in vascular dysfunction and vascular disease. *Biochemical Pharmacology* vol. 78 539–552 (2009).
4. Vasse, M. *et al.* Oncostatin M Induces Angiogenesis In Vitro and In Vivo. *Arterioscler. Thromb. Vasc. Biol.* **19**, (1999).
5. Nagata, T. *et al.* Oncostatin M, an interleukin-6 family cytokine, upregulates matrix metalloproteinase-9 through the mitogen-activated protein kinase kinase-extracellular signal-regulated kinase pathway in cultured smooth muscle cells. *Arterioscler. Thromb. Vasc. Biol.* **23**, 588–593 (2003).
6. Albasanz-Puig, A. *et al.* Oncostatin M is expressed in atherosclerotic lesions: a role for Oncostatin M in the pathogenesis of atherosclerosis. *Atherosclerosis* **216**, 292–8

(2011).
7. Zhang, X. *et al.* Oncostatin M receptor β deficiency attenuates atherogenesis by inhibiting JAK2/STAT3 signaling in macrophages. *J. Lipid Res.* **58**, 895–906 (2017).
8. Van Keulen, D. *et al.* Inflammatory cytokine oncostatin M induces endothelial activation in macro-and microvascular endothelial cells and in APOE*3Leiden.CETP mice. (2018) doi:10.1371/journal.pone.0204911.
9. van Keulen, D. *et al.* Oncostatin M reduces atherosclerosis development in APOE3Leiden.CETP mice and is associated with increased survival probability in humans. *PLoS One* **14**, (2019).
10. Brown, T. J., Lioubin, M. N. & Marquardt, H. Purification and characterization of cytostatic lymphokines produced by activated human T lymphocytes. Synergistic antiproliferative activity of transforming growth factor beta 1, interferon-gamma, and oncostatin M for human melanoma cells. *J. Immunol.* **139**, 2977–83 (1987).
11. Kastl, S. P. *et al.* In human macrophages the complement component C5a induces the expression of oncostatin M via AP-1 activation. *Arterioscler. Thromb. Vasc. Biol.* **28**, 498–503 (2008).
12. Grenier, A. *et al.* Oncostatin M Production and Regulation by Human Polymorphonuclear Neutrophils. *Blood* **93**, 1413–1421 (1999).
13. Tanaka, M. & Miyajima, A. Oncostatin M, a multifunctional cytokine. *Reviews of physiology, biochemistry and pharmacology* vol. 149 39–52 (2003).
14. Dey, G. *et al.* Signaling network of Oncostatin M pathway. *J. Cell Commun. Signal.* **7**, 103–108 (2013).
15. Mosley, B. *et al.* Dual oncostatin M (OSM) receptors. Cloning and characterization of an alternative signaling subunit conferring OSM-specific receptor activation. *J. Biol. Chem.* **271**, 32635–32643 (1996).
16. Takata, F. *et al.* Oncostatin M induces functional and structural impairment of blood–brain barriers comprised of rat brain capillary endothelial cells. *Neurosci. Lett.* **441**, 163–166 (2008).
17. Guihard, P. *et al.* Induction of osteogenesis in mesenchymal stem cells by activated monocytes/macrophages depends on oncostatin M signaling. *Stem Cells* **30**, 762–772 (2012).
18. Virmani, R. *et al.* Atherosclerotic Plaque Progression and Vulnerability to Rupture Angiogenesis as a Source of Intraplaque Hemorrhage Plaque Rupture Is the Dominant Cause of Acute Coronary Thrombosis. (2005) doi:10.1161/01.ATV.0000178991.71605.18.
19. Hutcheson, J. D., Maldonado, N. & Aikawa, E. Small entities with large impact: Microcalcifications and atherosclerotic plaque vulnerability. *Current Opinion in Lipidology* vol. 25 327–332 (2014).
20. Scaffidi, A. K. *et al.* Oncostatin M stimulates proliferation, induces collagen production and inhibits apoptosis of human lung fibroblasts. *Br. J. Pharmacol.* **136**, 793–801 (2002).
21. Shrivastava, R. *et al.* M2 polarization of macrophages by Oncostatin M in hypoxic tumor microenvironment is mediated by mTORC2 and promotes tumor growth and metastasis. *Cytokine* (2018) doi:10.1016/j.cyto.2018.03.032.
22. Van Der Wal, A. C. & Becker, A. E. Atherosclerotic plaque rupture - Pathologic basis of plaque stability and instability. *Cardiovascular Research* vol. 41 334–344 (1999).
23. Lonsdale, J. *et al.* The Genotype-Tissue Expression (GTEx) project. *Nat. Genet.* **45**, 580–585 (2013).
24. Grundberg, E. *et al.* Mapping cis-and trans-regulatory effects across multiple tissues in twins. *Nat. Genet.* **44**, 1084–1089 (2012).
25. Verhoeven, B. *et al.* Carotid atherosclerotic plaques in patients with transient ischemic attacks and stroke have unstable characteristics compared with plaques in asymptomatic and amaurosis fugax patients. *J. Vasc. Surg.* **42**, 1075–1081 (2005).

26. Van Der Laan, S. W. *et al.* Variants in ALOX5, ALOX5AP and LTA4H are not associated with atherosclerotic plaque phenotypes: The Athero-Express Genomics Study. *Atherosclerosis* **239**, 528–538 (2015).
27. O'Connell, J. *et al.* A General Approach for Haplotype Phasing across the Full Spectrum of Relatedness. *PLoS Genet.* **10**, 1004234 (2014).
28. Auton, A. *et al.* A global reference for human genetic variation. *Nature* vol. 526 68–74 (2015).
29. Francioli, L. C. *et al.* Whole-genome sequence variation, population structure and demographic history of the Dutch population. *Nat. Genet.* **46**, 818–825 (2014).
30. Verhoeven, B. A. N. *et al.* Athero-express: Differential atherosclerotic plaque expression of mRNA and protein in relation to cardiovascular events and patient characteristics. Rationale and design. *Eur. J. Epidemiol.* **19**, 1127–1133 (2004).
31. Van Lammeren, G. W. *et al.* Time-dependent changes in atherosclerotic plaque composition in patients undergoing carotid surgery. *Circulation* **129**, 2269–2276 (2014).
32. Hellings, W. E. *et al.* Intraobserver and interobserver variability and spatial differences in histologic examination of carotid endarterectomy specimens. *J. Vasc. Surg.* **46**, 1147–1154 (2007).
33. Hashimshony, T., Wagner, F., Sher, N. & Yanai, I. CEL-Seq: Single-Cell RNA-Seq by Multiplexed Linear Amplification. *Cell Rep.* **2**, 666–673 (2012).
34. Hashimshony, T. *et al.* CEL-Seq2: Sensitive highly-multiplexed single-cell RNA-Seq. *Genome Biol.* **17**, 77 (2016).
35. Ferraz, M. A. M. M. *et al.* An oviduct-on-a-chip provides an enhanced in vitro environment for zygote genome reprogramming. *Nat. Commun.* **9**, 1–14 (2018).
36. Li, H. & Durbin, R. Fast and accurate short read alignment with Burrows–Wheeler transform. *Bioinformatics* **25**, 1754–1760 (2009).
37. Morgan, M., Obenchain, V., Hester, J. & Pages, H. SummarizedExperiment. *The Visual Computer* vol. 24 (2020).
38. Love, M. I., Huber, W. & Anders, S. Moderated estimation of fold change and dispersion for RNA-seq data with DESeq2. *Genome Biol.* **15**, 550 (2014).
39. Box, G. E. P. & Cox, ; D R. *An Analysis of Transformations*. *Journal of the Royal Statistical Society. Series B (Methodological)* vol. 26 (1964).
40. Marchini, J., Howie, B., Myers, S., McVean, G. & Donnelly, P. A new multipoint method for genome-wide association studies by imputation of genotypes. *Nat. Genet.* **39**, 906–913 (2007).
41. Thoma, B., Bird, T. A., Friend, D. J., Gearing, D. P. & Dower, S. K. Oncostatin M and leukemia inhibitory factor trigger overlapping and different signals through partially shared receptor complexes. *J. Biol. Chem.* **269**, 6215–22 (1994).
42. Hermanns, H. *et al.* Contributions of leukemia inhibitory factor receptor and oncostatin M receptor to signal transduction in heterodimeric complexes with glycoprotein 130 - PubMed. *J Immunol* **163**, 6651–6658 (1999).
43. Rolfe, B. *et al.* Leukaemia inhibitory factor retards the progression of atherosclerosis. *Cardiovasc. Res.* **58**, 222–230 (2003).
44. van Setten, J. *et al.* Genome-wide association study of coronary and aortic calcification implicates risk loci for coronary artery disease and myocardial infarction. *Atherosclerosis* **228**, 400–405 (2013).
45. Nelson, C. P. *et al.* Association analyses based on false discovery rate implicate new loci for coronary artery disease. *Nat. Genet.* **49**, 1385–1391 (2017).
46. Malik, R. *et al.* Publisher correction: Multiancestry genome-wide association study of 520,000 subjects identifies 32 loci associated with stroke and stroke subtypes(Nature Genetics, (2018) 50, 4, (524-537), 10.1038/s41588-018-0058-3). *Nature Genetics* vol. 51 1192–1193 (2019).
47. Gu, W. *et al.* ICAM-1 regulates macrophage polarization by suppressing MCP- 1

expression via miR-124 upregulation. *Oncotarget* **8**, 111882–111901 (2017).
48. Barrett, T. J. Macrophages in Atherosclerosis Regression. *Arteriosclerosis, thrombosis, and vascular biology* vol. 40 20–33 (2020).
49. Matsuda, M. *et al.* Oncostatin M causes liver fibrosis by regulating cooperation between hepatic stellate cells and macrophages in mice. *Hepatology* **67**, 296–312 (2018).
50. Mozaffarian, A. *et al.* Mechanisms of Oncostatin M-Induced Pulmonary Inflammation and Fibrosis. *J. Immunol.* **181**, 7243–7253 (2008).

Table 1: Baseline characteristics of genotyped CEA patients from the Athero-Express Biobank Study.

Cerebrovascular disease history is defined by ischemic stroke prior to surgery. Coronary artery disease history includes coronary artery disease, myocardial infarction, percutaneous coronary intervention, and coronary artery bypass graft. Peripheral disease history includes diagnosed peripheral arterial occlusive disease, femoral artery interventions, and ankle-brachial index <70. Type 2 diabetes mellitus includes all individuals with diagnosed type 2 diabetes mellitus and those on appropriate medication. Hypertension includes all individuals with self-reported hypertension. Current smokers include all individuals smoking up to 6 months until the surgery date. BMI, kg/m^2. eGFR rate was based on the Modification of Diet in Renal Disease formula, mL/min/1.73m^2. Anti-hypertensives include all anti-hypertension medication. Anti-thrombotics include clopidogrel, dipyridamole, acenocoumarol, ascal, and anti-platelet drugs. Missingness shows the percentage of the patients of which we lack information on the specific patient characteristic.

Patient characteristics		**Missingness (%)**
Sex, male, n (%)	976 (64.0)	5.7
Age in years, mean (SD)	68.84 (9.33)	5.7
History		
Cerebrovascular disease, n (%)	478 (33.2)	5.7
Coronary artery disease, n (%)	430 (29.9)	5.8
Peripheral artery disease, n (%)	297 (20.7)	5.8
Risk factors		
Type 2 diabetes mellitus, n (%)	332 (23.1)	5.7
Hypertension, n (%)	1017 (73.0)	8.7
Current smoker, n (%)	492 (34.9)	7.5
BMI, median [IQR]	26.0 [24.0-28.4]	11.5
eGFR, median [IQR]	72.3 [58.7-85.4]	8.1
Total cholesterol in mmol/L, median [IQR]	4.38 [3.60-5.25]	22.8

LDL in mmol/L, median [IQR]	2.40 [1.81-3.13]	27.8
HDL in mmol/L, median [IQR]	1.06 [0.87-1.30]	25.0
Triglycerides in mmol/L, median [IQR]	1.50 [1.08-2.04]	24.6
Medication		
Antihypertensives, n (%)	1110 (77.2)	5.8
Lipid lowering drugs, n (%)	1112 (77.4)	5.8
Antithrombotics, n (%)	1272 (88.6)	6.0
Symptoms		
Asymptomatics, n (%)	195 (13.6)	6.0
Ocular, n (%)	221 (15.4)	6.0
TIA, n (%)	634 (44.2)	6.0
Stroke, n (%)	384 (26.8)	6.0

Table 2: *OSMR* and *LIFR* variants and their association with plaque phenotypes. For each variant, the association with plaque phenotypes is given. NES: the normalized effect size on expression; Alleles: the effect allele and the other allele, respectively; EAF: effect allele frequency in the Athero-Express Biobank; Info: estimated imputation score in the Athero-Express Biobank; β: effect size; s.e.: standard error; *p*: p-value of association. Calcification and collagen were classified as no/minor vs moderate/heavy, fat content as 10% vs >10% fat of plaque area, intraplaque hemorrhage was classified as absent vs present. Smooth muscle cells and macrophages were classified as Box-Cox transformed percentage of plaque area and vessel density as Box-Cox transformed number of vessels/hotspot.

Gene	Variant	NES	Alleles	EAF	Info	Phenotype	β (s.e.)	*p*
OSMR	rs13168867	-0.13	C/T	0.393	0.999	Calcification	0.036 (0.077)	0.637
						Collagen	-0.259 (0.095)	6.22×10^{-3}
						Fat content	0.248 (0.088)	4.66×10^{-3}
						Intraplaque hemorrhage	-0.014 (0.080)	0.862
						Smooth muscle cells	0.001 (0.011)	0.913
						Vessel density	-1.06×10^{-4} (0.004)	0.976
						Macrophages	0.004 (0.015)	0.809
LIFR	rs10491509	0.29	A/G	0.351	0.989	Calcification	0.046 (0.082)	0.577

						Collagen	0.134 (0.104)	0.194
						Fat content	0.086 (0.094)	0.363
						Intraplaque hemorrhage	0.071 (0.086)	0.414
						Smooth muscle cells	-0.003 (0.012)	0.840
						Vessel density	0.002 (0.004)	0.577
						Macrophages	0.015 (0.016)	0.354

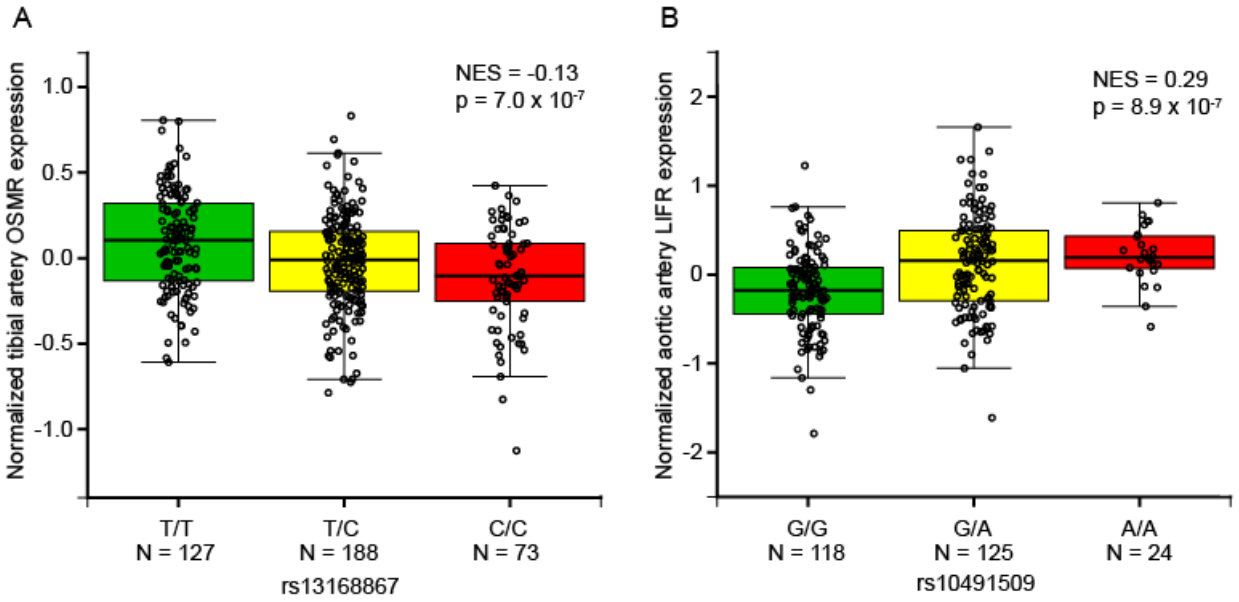

Figure 1: Association of *OSMR* and *LIFR* variants in non-diseased arterial tissues. Per variant, the normalized expression of *OSMR* (A) and *LIFR* (B) is given in non-diseased arterial tissue. Data from GTEx Portal (www.gtexportal.org). NES: Normalized effect size. In aortic arterial tissue, rs13168867 had a NES of -0.123 and in tibial arterial tissue, rs10491509 had a NES of 0.0881 (**Supplementary Figure 1** and **2**).

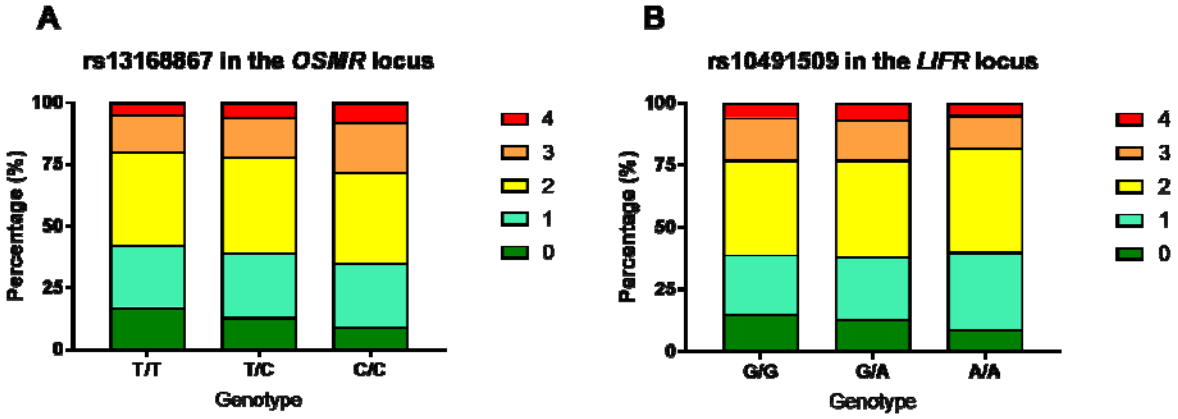

Gene	Variant	NES	Alleles	EAF	Info	β (s.e.)	*p*
OSMR	rs13168867	-0.13	C/T	0.393	0.999	0.118 (0.040)	**3.00×10^{-3}**
LIFR	rs10491509	0.29	A/G	0.351	0.989	0.001 (0.043)	0.981

Figure 2: Association of *OSMR* and *LIFR* variants with overall plaque vulnerability. The plaques were given a vulnerability score ranging from 0 (least vulnerable) to 4 (most vulnerable). The bars represent the proportion of each plaque score per genotype for rs13168867 in the *OSMR* locus (A) and rs10491509 in the *LIFR* locus (B). NES: normalized effect size on expression (GTEx Portal, www.gtexportal.org[23]); Alleles: the effect allele and the other allele, respectively; EAF: effect allele frequency in the Athero-Express Biobank; Info: estimated imputation score in the Athero-Express Biobank; β: effect size; s.e.: standard error; *p*: p-value of association.

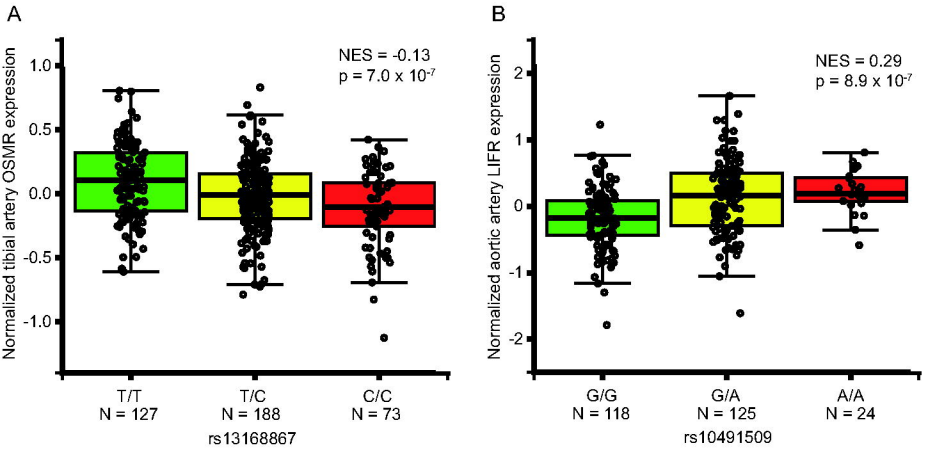
A
Normalized tibial artery OSMR expression
1.0
0.5
0.0
-0.5
-1.0
NES = -0.13
p = 7.0 x 10-7
T/T
N = 127
T/C
N = 188
C/C
N = 73
rs13168867
B
Normalized aortic artery LIFR expression
2
1
0
-1
-2
NES = 0.29
p = 8.9 x 10-7
G/G
N = 118
G/A
N = 125
A/A
N = 24
rs10491509

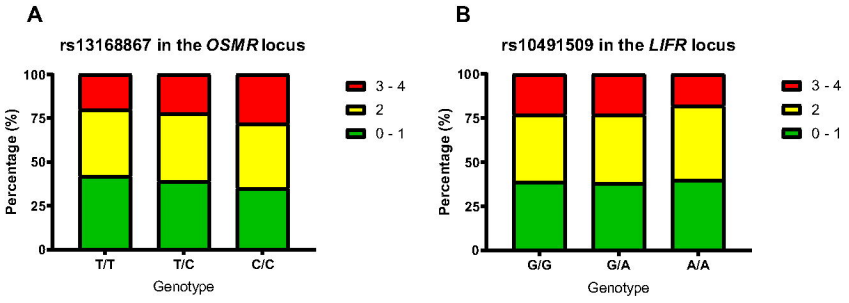

Gene	Variant	NES	Alleles	EAF	Info	β (s.e.)	*p*
OSMR	rs13168867	-0.13	C/T	0.393	0.999	0.118 (0.040)	**3.00×10^{-3}**
LIFR	rs10491509	0.29	A/G	0.351	0.989	0.001 (0.043)	0.981